A fragment of human TrpRS as a potent antagonist of ocular angiogenesis

Atsushi Otani*, Bonnie M. Slike†, Michael I. Dorrell*, John Hood‡, Karen Kinder*, Karla L. Ewalt†, David Cheresh‡, Paul Schimmel†§, and Martin Friedlander*§

*Department of Cell Biology, †The Skaggs Institute for Chemical Biology and the Department of Molecular Biology, and ‡Departments of Immunology and Vascular Biology, The Scripps Research Institute, La Jolla, CA 92037

Contributed by Paul Schimmel, November 9, 2001

Pathological angiogenesis contributes directly to profound loss of vision associated with many diseases of the eye. Recent work suggests that human tyrosyl- and tryptophanyl-tRNA synthetases (TrpRS) link protein synthesis to signal transduction pathways including angiogenesis. In this study, we show that a recombinant form of a COOH-terminal fragment of TrpRS is a potent antagonist of vascular endothelial growth factor-induced angiogenesis in a mouse model and of naturally occurring retinal angiogenesis in the neonatal mouse. The angiostatic activity is dose-dependent in both systems. The recombinant fragment is similar in size to one generated naturally by alternative splicing and can be produced by proteolysis of the full-length protein. In contrast, the full-length protein is inactive as an antagonist of angiogenesis. These results suggest that fragments of TrpRS, as naturally occurring and potentially nonimmunogenic anti-angiogenics, can be used for the treatment of neovascular eye diseases.

The vast majority of diseases that cause catastrophic loss of vision do so as a result of abnormal angiogenesis. Age-related macular degeneration affects 12–15 million Americans over the age of 65 and causes visual loss in 10–15% of them as a direct effect of choroidal (subretinal) neovascularization. The leading cause of visual loss for Americans under the age of 65 is diabetes mellitus. For example, 16 million individuals in the United States are diabetic, and 40,000 new patients per year suffer from ocular complications of the disease, often a result of retinal neovascularization (1). Although significant progress has been made in identifying factors that promote and inhibit angiogenesis, no treatment is currently available to specifically inhibit ocular neovascularization.

In the normal adult, angiogenesis (defined as the growth of new blood vessels from preexisting ones) is tightly regulated and limited to wound healing, pregnancy, and menstruation. Understanding of the molecular events involved in the angiogenic process has advanced significantly since the purification of the first angiogenic molecules nearly two decades ago (2). This process, under physiologic conditions, may be activated by specific angiogenic molecules such as basic and acidic fibroblast growth factor (3), vascular endothelial growth factor (VEGF) (4), angiogenin (5), transforming growth factor (6), and platelet-derived growth factor (7). Angiogenesis can also be suppressed by inhibitory molecules such as IFN-α (8), thrombospondin-1 (9), angiostatin (10), endostatin (11), hemopexin-like domain of matrix metalloproteinase 2 (PEX) (12), or pigment epithelial-derived factor (13). It is the balance of these naturally occurring stimulators and inhibitors that is thought to tightly control the normally quiescent capillary vasculature (14). When this balance is upset, as in certain disease states, capillary endothelial cells are induced to proliferate, migrate, and ultimately differentiate.

We have been investigating the angiostatic activity of fragments of tryptophanyl-tRNA synthetase (TrpRS). In addition to its conserved role in protein synthesis, recent work demonstrates that a natural alternative splice variant of TrpRS in human cells—mini TrpRS—has angiostatic activity (15). Production of this NH_2-terminally truncated variant is stimulated *in vitro* by IFN-γ in a variety of cells, including monocytes, keratinocytes, epithelial cells, primary human fibroblasts, and bladder transitional cell carcinomas (16–25), and is suppressed by transforming growth factor-β (25). Although both human full-length TrpRS and mini TrpRS are enzymatically active in aminoacylation, they differ in angiostatic activity. Only the shorter form, lacking an NH_2-terminal extension unique to TrpRS from higher eukaryotes, is active as an inhibitor of VEGF-induced angiogenesis (15). Thus, functional differentiation of human full-length TrpRS and mini TrpRS is generated by distinct protein expression profiles and by the presence or absence of an NH_2-terminal domain.

During earlier studies of the angiostatic activity of mini TrpRS, we found that two NH_2-terminally truncated forms of TrpRS were produced by digestion with the extracellular protease leukocyte elastase (15). Both proteolytic products contained the conserved core domain found in eukaryotic and prokaryotic TrpRS. The larger product, T1-TrpRS, was similar in size and angiostatic activity to mini TrpRS (15). In this study, we investigated the angiostatic activity of T2-TrpRS, the smaller proteolytic product in which the entire NH_2-terminal domain has been deleted. This fragment was tested in a model of VEGF-induced angiogenesis and on naturally occurring angiogenesis in the developing retina. In each system, T2-TrpRS exhibited potent, dose-dependent angiostatic activity. As a fragment of a naturally occurring gene product, T2-TrpRS would lend itself to local treatment in the eye by cell-based or gene therapy in physiologically relevant amounts.

Materials and Methods

Protein Production, Labeling, and Biochemical Analysis. The T2-TrpRS fragment of human full-length TrpRS was identified after cleavage with leukocyte elastase (Sigma) (15). The gene encoding human T2-TrpRS including a COOH-terminal six-histidine tag was cloned into plasmid pET20b and overexpressed in *Escherichia coli* strain BL21 (DE3, Novagen) by induction with 1 mM isopropyl β-D-thiogalactopyranoside for 2 h. Schematic alignment of human T2-TrpRS with full-length and other truncated human TrpRS is shown in Fig. 1. Full-length human TrpRS encodes residues 1–471, mini TrpRS residues 48–471, T1-TrpRS residues 74–471, and T2-TrpRS residues 94–471. The protein was purified on a nickel affinity column (Ni-NTA agarose, Qiagen, Chatsworth, CA) from the supernatant of lysed cells. Endotoxin was determined to be <0.01 endotoxin units/ml by a *Limulus* amebocyte lysate gel-clot assay (E-Toxate, Sigma). Protein concentration was determined by the Bradford assay with BSA (Sigma) as a standard (Bio-Rad).

Abbreviations: VEGF, vascular endothelial growth factor; TrpRS, tryptophanyl-tRNA synthetase; DAPI, 4′-6-diamidino-2-phenylindole.

§To whom reprint requests may be addressed. E-mail: friedlan@scripps.edu or schimmel@scripps.edu.

The publication costs of this article were defrayed in part by page charge payment. This article must therefore be hereby marked "*advertisement*" in accordance with 18 U.S.C. §1734 solely to indicate this fact.

www.pnas.org/cgi/doi/10.1073/pnas.012601899

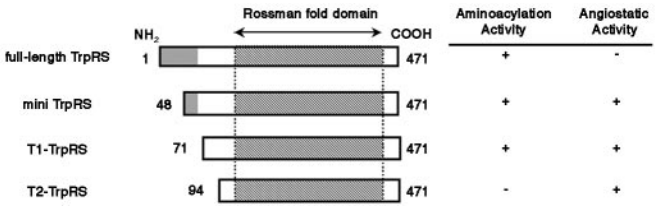

Fig. 1. Schematic representation of human TrpRS variants. Shaded regions of TrpRS represent the NH_2-terminal appended domain. Numbers on the left and right correspond to the NH_2- and COOH-terminal residues relative to the human full-length enzyme, respectively. The NH_2 domain of TrpRS has sequence similarity to the extra domains of human GluProRS (a fusion of glutamyl- and prolyl-tRNA synthetases), MetRS, GlyRS, and HisRS. TrpRS variants active (+) or inactive (−) in aminoacylation or angiogenesis inhibition assays are indicated (51–56).

Alexa Fluor 488 labeling of T2-TrpRS or TrpRS was performed with an Alexa Fluor 488 protein labeling kit (Molecular Probes) according to the manufacturer's instructions. The extent of labeling was between 1.0 and 1.4 mol of Alexa Fluor 488 per mol of T2-TrpRS and 1.9 mol of Alexa Fluor 488 per mol of TrpRS.

Matrigel Angiogenesis Assay. The mouse Matrigel angiogenesis assay was used to examine the angiostatic activity of T2-TrpRS (26, 27). It was performed as described with the following modifications (27). Athymic wehi mice were implanted with 400 μl of growth factor-depleted Matrigel (Becton Dickinson) containing 20 nM VEGF. The angiostatic activity of T2-TrpRS was initially tested by including 2.5 μM T2-TrpRS in the Matrigel plug. The potency was determined by including various concentrations of T2-TrpRS in the plug. On day 5, the mice were intravenously injected with the fluorescein-labeled endothelial binding lectin *Griffonia* (*Bandeiraea*) *simplicifolia* I, isolectin B4 (Vector Laboratories, Burlingame, CA), and the Matrigel plugs were resected. The fluorescein content of each plug was quantified by spectrophotometric analysis after grinding the plug in RIPA buffer (10 mM sodium phosphate, pH 7.4/150 mM sodium chloride/1% Nonidet P-40/0.5% sodium deoxycholate/0.1% SDS).

Postnatal Mouse Retinal Angiogenesis Assay. An *in vivo* angiogenesis assay in the postnatal mouse (BALB/c, The Jackson Laboratory) was used to evaluate the angiostatic activity of T2-TrpRS. This model will be discussed further below. Intravitreous injection and retina isolation was performed with a dissecting microscope (SMZ 645, Nikon). An eyelid fissure was created in postnatal day 7 (P7) mice with a fine blade to expose the globe for injection of T2-TrpRS (5 pmol) or TrpRS (5 pmol). The samples (0.5 μl) were injected with a Hamilton syringe fitted with a 32-gauge needle. The injection was made between the equator and the corneal limbus; during injection the location of the needle tip was monitored by direct visualization to determine that it was in the vitreal cavity. Eyes with needle-induced lens or retinal damage were excluded from the study. After the injection, the eyelids were repositioned to close the fissure.

On postnatal day 12 (P12), animals were euthanized and eyes enucleated. After 10 min in 4% paraformaldehyde, the cornea, lens, sclera, and vitreous were excised through a limbal incision. The isolated retina was prepared for staining by soaking in methanol for 10 min on ice, followed by blocking in 50% FBS (GIBCO) with 20% normal goat serum (The Jackson Laboratory) in PBS for 1 h on ice. The blood vessels were specifically visualized by staining the retina with a rabbit anti-mouse collagen IV antibody (Chemicon) (28, 29) diluted 1:200 in blocking buffer for 18 h at 4°C. An Alexa Fluor 594-conjugated goat anti-rabbit IgG antibody (Molecular Probes, 1:200 dilution in blocking buffer) was incubated with the retina for 2 h at 4°C. The retinas were mounted with slow-fade mounting media (Molecular Probes).

Angiostatic activity was evaluated based on the degree of angiogenesis in the deep, outer retinal vascular layer (secondary layer) that forms between P8 and P12. The appearance of the inner blood vessel network (primary layer) was evaluated for normal development and signs of toxicity. None of the protein constructs used in this study produced any adverse effects on the primary layer.

Localization of T2-TrpRS Binding within the Retina. To assess the uptake and localization of T2-TrpRS injected into the retina, Alexa 488-labeled T2-TrpRS was injected into the vitreous of the eye on postnatal day 7 (P7). Globes were harvested on P8 and P12 and fixed in 4% paraformaldehyde for 15 min. The retinas were further dissected free of adherent nonretinal tissue and placed in 4% paraformaldehyde overnight at 4°C and then embedded in medium (Tissue-Tek OCT, Sakura FineTechnical) on dry ice. Cryostat sections (10 μm) were rehydrated with PBS and blocked with 5% BSA, 2% normal goat serum in PBS. Blood vessels were visualized with anti-mouse collagen IV antibody as described above. Vectashield containing 4′-6-diamidino-2-phenylindole (DAPI) nuclear stain (Vector Laboratories) was used to mount the tissues with a coverslip.

Alternatively, unstained retina sections were incubated with 200 nM Alexa 488-labeled full-length TrpRS or Alexa 488-labeled T2 in blocking buffer overnight at 4°C. Sections were washed six times for 5 min each in PBS, followed by incubation with 1 μg/ml DAPI for 5 min for visualization of the nuclei. Preblocking with unlabeled T2-TrpRS was performed by incubating 1 μM unlabeled T2-TrpRS for 8 h at 4°C before incubation with Alexa 488-labeled T2-TrpRS.

Confocal Microscopy. Retinas were examined with a multiphoton Bio-Rad MRC1024 confocal microscope. Three-dimensional vascular images were produced from a set of Z-series images by using CONFOCAL ASSISTANT (Bio-Rad).

Results

T2 TrpRS Fragment. During earlier studies of a naturally occurring, truncated variant of TrpRS (designated mini TrpRS), we found that it exhibited angiostatic activity *in vitro* and *in vivo*. Similarly, T1-TrpRS (a truncated TrpRS produced by leukocyte elastase digestion), which is close in size to mini TrpRS, also had angiostatic activity (15). A shorter proteolytic product, T2-TrpRS, was isolated from the leukocyte elastase digestion of human TrpRS (Fig. 1). The NH_2 terminus of T2-TrpRS began at Ser-94 as deduced by protein sequencing. Western blot analysis indicated that the COOH terminus was intact, as it contained the His_6-tag fused to the recombinant protein. Compared with mini TrpRS, T2-TrpRS had a larger NH_2-terminal deletion and thus completely lacked the NH_2-terminal appended domain unique to higher eukaryotic TrpRS (Fig. 1). Despite the more extensive NH_2-terminal deletion and loss of enzymatic activity, T2-TrpRS contains the Rossmann fold nucleotide-binding domain conserved throughout all prokaryotic and eukaryotic TrpRS. Whereas full-length TrpRS, mini TrpRS, and T1-TrpRS variants all retained aminoacylation activity, T2-TrpRS was inactive for aminoacylation (Fig. 1).

Angiostatic Potency of T2-TrpRS in the Mouse Matrigel Plug Assay. We examined T2-TrpRS to determine whether it had angiostatic activity, even though it had lost aminoacylation activity. The mouse Matrigel assay was used to examine the angiostatic activity of T2-TrpRS *in vivo* (27). $VEGF_{165}$ induces the development of blood vessels into the mouse Matrigel plug. When

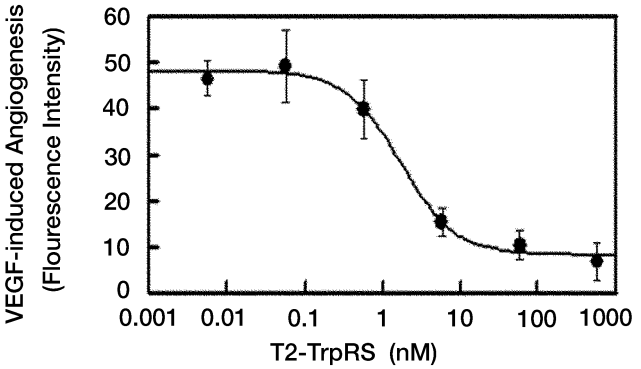

Fig. 2. Activity of T2-TrpRS in the murine Matrigel model of angiogenesis. Athymic wehi mice were subcutaneously implanted with 400 μl of growth factor-depleted Matrigel containing VEGF and T2-TrpRS. On day 5, the mice were intravenously injected with the fluorescein-labeled endothelial binding lectin *Griffonia* (*Bandeiraea*) *simplicifolia* I, isolectin B4. The plugs were resected and solubilized, and the fluorescein content was quantified by spectrometry. The graph plots relative fluorescein content of resected Matrigel plugs treated with $VEGF_{165}$ (20 nM) and increasing concentrations of T2-TrpRS.

T2-TrpRS was added to the Matrigel along with $VEGF_{165}$, angiogenesis was blocked in a dose-dependent manner, with an IC_{50} of 1.7 nM (Fig. 2).

Postnatal Mouse Retinal Angiogenesis Model. Immediately after birth (P0), retinal vasculature is virtually absent in the mouse. By 2 weeks postnatal (P14), the retina has attained an adult pattern of retinal vessels coincident with the onset of vision. Physiological neovascularization of the retina occurs during this period via a stereotypical, biphasic developmental pattern of angiogenesis. Initially, spoke-like peripapillary vessels grow radially from the central retinal artery and vein, becoming progressively interconnected by a capillary plexus that forms between them. This superficial vascular layer grows centrifugally in area, volume, and complexity as a monolayer within the nerve fiber layer during the first 9–10 days following birth. Administration of intravitreal PBS or control compounds did not prevent normal vascular development.

The second phase of retinal vessel formation begins between postnatal days 8 (P8) and 10 (P10) when sprouts from capillaries of the superficial (primary) vascular layer penetrate into the retina, where their tips branch and anastamose laterally to form a planar deep (secondary) vascular layer. Whereas the secondary layer is in place by P14, it undergoes extensive remodeling from P14 to P21. The formation of these vascular networks in the neonatal mouse is strikingly similar to the events occurring in the third trimester human fetus (30). The reproducibility of this process and its easy accessibility in postnatal animals provide an opportunity to evaluate the angiostatic effect of putative antagonists of angiogenesis. Qualitative evaluation is accomplished by photographing the primary and secondary layers and determining the percentage of eyes in which formation of the secondary layer is completely or partially inhibited. This evaluation minimizes the bias associated with a subjective scoring system and provides an objective endpoint for comparison of various compounds.

Effects of T2-TrpRS on Retinal Angiogenesis. Endotoxin-free full-length TrpRS, mini TrpRS (48-kDa splice variant of TrpRS), and T2-TrpRS (43-kDa cleavage product of TrpRS) were prepared as recombinant proteins. These proteins were injected intravitreally into neonatal mice on postnatal day 7 or 8, and the retinas were harvested on P12 or P13. Anti-mouse collagen IV antibody and fluorescein-conjugated secondary antibody were used to visualize the vessels in retinal whole mount preparations.

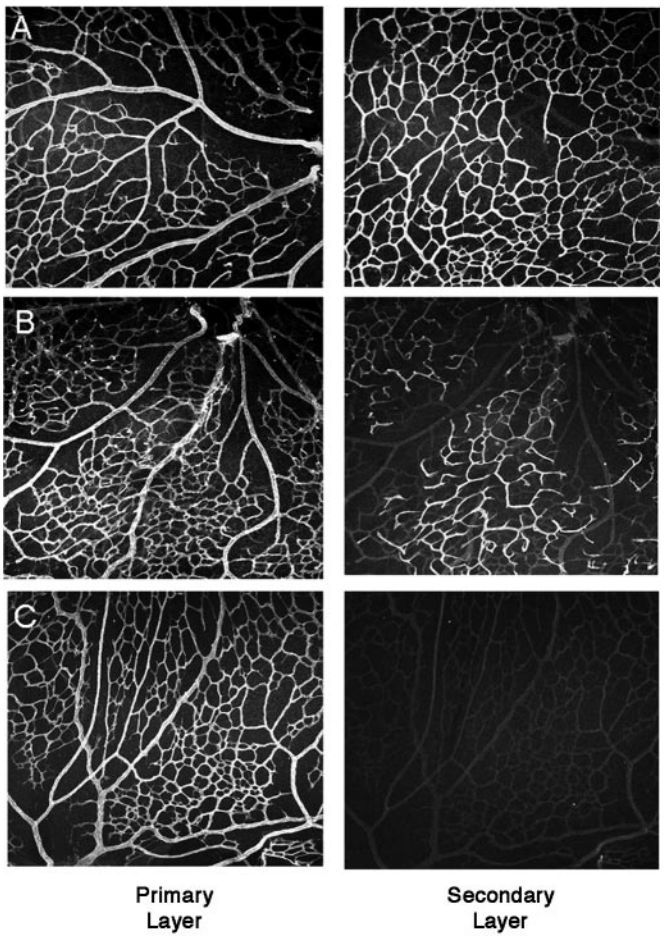

Fig. 3. Activities of human TrpRS constructs on postnatal mouse retinal vascular development. Representative images taken on postnatal day 12 of primary (*Left*) and secondary (*Right*) retinal vascular layers 4 days after intravitreous injection (0.5 μl of protein per eye at P7) of full-length TrpRS (*A*), mini TrpRS (*B*), or T2−TrpRS (*C*). Vessels were stained with an anti-collagen IV antibody. (*C Right*) The dim vascular image is ''bleed through'' from the overlying primary layer. The secondary network observed in the right panels in *A* and *B* is much brighter and appears as brightly stained vessels in an intercalated network.

Anti-angiogenic activity was evaluated based on the effect of injected proteins on formation of the secondary vascular layer (Fig. 3). Complete inhibition of the secondary vascular layer was observed in 8.2% (n = 73) of PBS-treated eyes (Fig. 4). In contrast, complete inhibition of the outer network was observed in 28% of mini TrpRS (5 pmol) treated eyes (n = 75). The smaller T2-TrpRS variant was far more potent, with dose-dependent activity; 14.3% were completely inhibited after treatment with 1 pmol of T2-TrpRS (n = 14), 40% after treatment with 2.5 pmol (n = 20), and 69.1% after 5 pmol (n = 20). In contrast, addition of 5.0 pmol of full-length TrpRS had no effect on the development of the secondary layer.

Alexa 488-Labeled T2-TrpRS Localizes to Retinal Blood Vessels. To visualize the intraocular localization of T2-TrpRS, we examined the distribution of Alexa 488-labeled T2-TrpRS following intravitreous injection on postnatal day 7. Retinas were isolated the following day, sectioned, and examined by using confocal microscopy. The distribution of the injected protein was restricted to blood vessels. This localization was confirmed by costaining

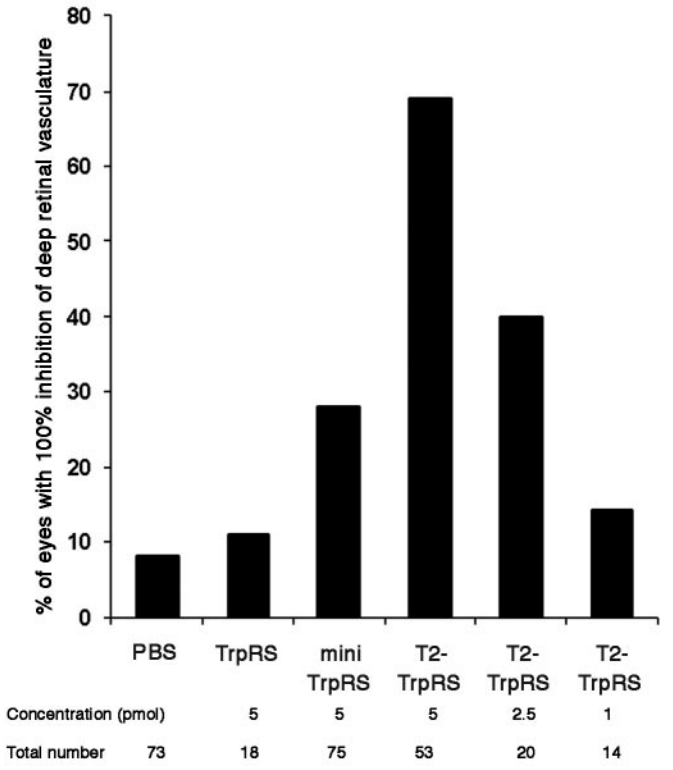

Fig. 4. Angiostatic effect of human TrpRS in postnatal mouse retinal angiogenesis model. The data are presented as the percentage of complete inhibition of deep vascular (secondary layer) in each sample. PBS, $n = 73$; full-length TrpRS (5 pmol), $n = 18$; mini TrpRS (5 pmol), $n = 75$; T2-TrpRS (5 pmol), $n = 53$; T2-TrpRS (2.5 pmol), $n = 20$; and T2-TrpRS (1 pmol), $n = 14$.

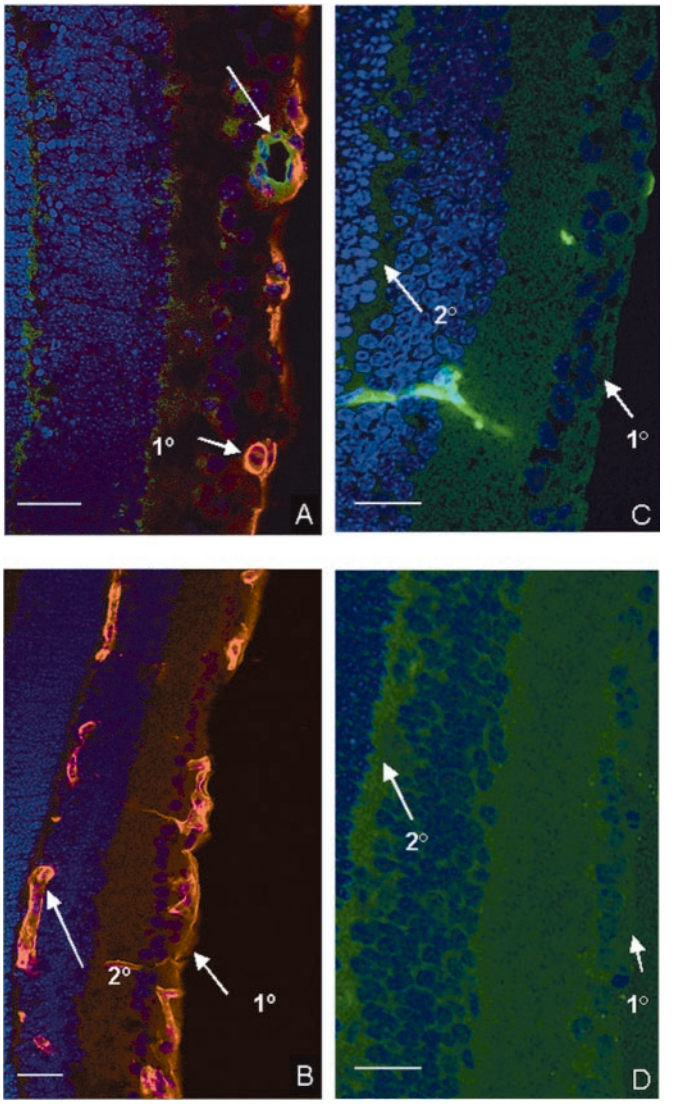

Fig. 5. Alexa 488-labeled T2-TrpRS is angiostatic and localizes to retinal blood vessels. Alexa 488-labeled T2-TrpRS (*A*) or full-length TrpRS (*B*) were injected (0.5 μl, intravitreous) on postnatal day 7 (P7). The retinas were harvested on P8 and stained with an anti-collagen IV antibody and DAPI nuclear stain. Labeled T2-TrpRS (arrow pointing to green vessel in *A*) localized to blood vessels in the primary superficial network (1°). Note that the secondary deep network is completely absent (2°). Whereas both the primary (1°) and secondary (2°) vascular layers are present in eyes injected with Alexa 488-labeled full-length TrpRS (arrows in *B*), no labeling is observed. In a separate set of experiments, frozen sections of P15 retinas were stained with Alexa 488-labeled T2-TrpRS (*C*) or Alexa 488-labeled full-length TrpRS (*D*) and imaged by confocal scanning laser microscopy. Labeled T2-TrpRS selectively localized to blood vessels and appears as a green penetrating vessel between the primary and secondary retinal vascular layers (*C*). No staining was observed with full-length TrpRS (*D*). Green, Alexa 488-labeled proteins; red, collagen IV-stained retinal vessels; blue, nuclei.

labeled T2-TrpRS-treated eyes with an Alexa 594-labeled anti-collagen IV antibody (data not shown). Five days after injection of Alexa 488-labeled T2-TrpRS (on P12), the green fluorescence of the labeled T2-TrpRS was still visible (Fig. 5*A*). In these retinas, no secondary vascular layer was observed at P12, indicating that the Alexa 488-labeled T2-TrpRS retained angiostatic activity comparable to unlabeled T2-TrpRS. Retinas injected on P7 with Alexa 488-labeled full-length TrpRS developed a secondary vascular layer by P12, but no vascular staining was observed (Fig. 5*B*).

To further evaluate the binding properties of labeled T2-TrpRS, cross-sectioned slices of normal neonatal retinas were stained with Alexa 488-labeled T2-TrpRS. Under these conditions, Alexa 488-labeled T2-TrpRS only bound to vessels (Fig. 5*C*). The binding was specific as it was blocked by preincubation with unlabeled T2-TrpRS (data not shown). No retinal staining was observed when Alexa 488-labeled full-length TrpRS was applied to the retinas (Fig. 5*D*), consistent with the absence of angiostatic activity of the full-length enzyme.

Discussion

Full-length TrpRS contains a unique NH_2-terminal domain and lacks angiostatic activity. Removing part or all of this entire domain reveals a protein with angiostatic activity. The structures responsible for angiostatic activity of T2-TrpRS seem to be contained within the core Rossmann fold nucleotide binding domain. The NH_2-terminal domain, which can be deleted by alternative splicing or by proteolysis, may regulate the angiostatic activity of TrpRS, possibly by revealing a binding site necessary for angiostasis that is inaccessible in full-length TrpRS.

VEGF-induced angiogenesis in the mouse Matrigel model was completely inhibited by T2-TrpRS, as was physiological angiogenesis in the neonatal retina. Interestingly, the most potent anti-angiogenic effect of TrpRS fragments *in vitro* and in chicken chorioallantoic membrane and Matrigel models is observed in VEGF-stimulated angiogenesis. The neonatal mouse retinal angiogenesis results are consistent with a link between VEGF-stimulated angiogenesis and the angiostatic effects of TrpRS fragments; retinal angiogenesis in this system may be driven by

VEGF (31, 32). In addition, the inhibition observed in the retinal model was specific for newly developing vessels; preexisting (at the time of injection) primary vascular layer vessels were unaltered by the treatment. Although the mechanism for the angiostatic activity of T2-TrpRS is not known, the specific localization of T2-TrpRS to the retinal endothelial vasculature and the selective effect of T2-TrpRS on newly developing blood vessels suggest that T2-TrpRS may function through an endothelial cell receptor expressed on proliferating or migrating cells. Further understanding of the mechanism of T2-TrpRS angiostatic activity requires identification of the relevant cell receptor.

A variety of cell types that produce, with IFN-γ stimulation, the angiostatic mini TrpRS also produce angiostatic factors such as IP-10 (15). Thus, these results raise the possibility of a role for TrpRS in normal, physiologically relevant pathways of angiogenesis. Another ubiquitous cellular protein, pro-EMAPII (p43), has two apparently unrelated roles similar to these reported here for TrpRS. Pro-EMAPII assists protein translation by associating with the multisynthetase complex of mammalian aminoacyl tRNA synthetases (33, 34). It is processed and secreted as EMAPII (35–41), and a role for EMAPII as an angiostatic mediator during lung development has been suggested (42).

Thus, T2-TrpRS might be used in physiologically relevant angiogenic remodeling observed under normal or pathological conditions. In normal angiogenesis, T2-TrpRs could be critical for establishing physiologically important avascular zones present in some organs such as the foveal avascular zone of the central retina. Pathological angiogenesis could occur if the cleavage of full-length TrpRS was inhibited, leading to an overgrowth of vessels.

In ocular diseases, neovascularization can lead to catastrophic loss of vision (43–45). These patients may receive great benefit from therapeutic inhibition of angiogenesis. Vascular endothelial growth factor has been associated with neovascularization and macular edema in the retina (14, 46), although it is believed that other angiogenic stimuli also have roles in retinal angiogenesis (29, 47). In this study, we have observed an association between VEGF-stimulated angiogenesis and potent angiostatic activity of TrpRS fragments, suggesting that these molecules may be useful in the treatment of hypoxic and other proliferative retinopathies. A variety of inhibitors using different strategies have been described in the literature. These include direct inhibition of endothelial cell proliferation with TNP-470 (48), thrombospondin-1 (49), angiostatin and endostatin (11), interruption of endothelial cell adhesion and migration with anti-$\alpha_V\beta_3$ integrin antibody LM609 (50), and inhibition of proteases with fragments of MMPs (12).

Although it is difficult to directly compare the potency of T2-TrpRS to these other angiostatic agents without using the identical angiogenesis assays, we have not previously observed in any assay an anti-angiogenic agent that completely inhibits angiogenesis 70% of the time as does the T2-TrpRS (Fig. 5). Another potential advantage of TrpRS fragments is that they represent naturally occurring and, therefore, potentially nonimmunogenic anti-angiogenics. Thus, these molecules can be delivered via targeted cell- or viral vector-based therapy. Because many patients with neovascular eye diseases have associated systemic ischemic disease, local anti-angiogenic treatment with genetically engineered cells or viral vectors placed directly into the eye is desirable. We are currently using T2-TrpRS in such approaches to develop better delivery systems to treat such diseases of the posterior segment.

We thank Dr. Lois Smith for providing helpful comments on the manuscript, Drs. Faith Barnett, Sheila Fallon, Ray Gariano, and Matthew Ritter for useful discussions during the course of this work, and Stacey Hanekamp and Suzanne Bacon for assistance in preparing the manuscript. This work was supported by National Institutes of Health Grants EY12599 (to M.F.) and GM23652 and CA92577 (to P.S.). Additional support came from The Robert Mealey Program for the Study of Macular Degenerations (to M.F.) and fellowships from the Achievement Rewards for College Scientists Foundation, San Diego Chapter (to M.D.) and the National Foundation for Cancer Research (to P.S.).

1. Aiello, L. P., Gardner, T. W., King, G. L., Blankenship, G., Cavallerano, J. D., Ferris, F. L. & Klein, R. (1998) *Diabetes Care* **21,** 143–156.
2. Shing, Y., Folkman, J., Sullivan, R., Butterfield, C., Murray, J. & Klagsbrun, M. (1984) *Science* **223,** 1296–1299.
3. Folkman, J. (1992) *Semin. Cancer Biol.* **3,** 65–71.
4. Ferrara, N., Houck, K., Jakeman, L. & Leung, D. W. (1992) *Endocr. Rev.* **13,** 18–32.
5. Fett, J. W., Strydom, D. J., Lobb, R. R., Alderman, E. M., Bethune, J. L., Riordan, J. F. & Vallee, B. L. (1985) *Biochemistry* **24,** 5480–5486.
6. Antonelli-Orlidge, A., Saunders, K. B., Smith, S. R. & D'Amore, P. A. (1989) *Proc. Natl. Acad. Sci. USA* **86,** 4544–4548.
7. Ishikawa, F., Miyazono, K., Hellman, U., Drexler, H., Wernstedt, C., Hagiwara, K., Usuki, K., Takaku, F., Risau, W. & Heldin, C. H. (1989) *Nature (London)* **338,** 557–562.
8. Ezekowitz, R. A., Mulliken, J. B. & Folkman, J. (1992) *N. Engl. J. Med.* **326,** 1456–1463.
9. Tolsma, S. S., Volpert, O. V., Good, D. J., Frazier, W. A., Polverini, P. J. & Bouck, N. (1993) *J. Cell Biol.* **122,** 497–511.
10. Derynck, R. (1990) *Mol. Reprod. Dev.* **27,** 3–9.
11. O'Reilly, M. S., Boehm, T., Shing, Y., Fukai, N., Vasios, G., Lane, W. S., Flynn, E., Birkhead, J. R., Olsen, B. R. & Folkman, J. (1997) *Cell* **88,** 277–285.
12. Brooks, P. C., Silletti, S., von Schalscha, T. L., Friedlander, M. & Cheresh, D. A. (1998) *Cell* **92,** 391–400.
13. Dawson, D. W., Volpert, O. V., Gillis, P., Crawford, S. E., Xu, H., Benedict, W. & Bouck, N. P. (1999) *Science* **285,** 245–248.
14. D'Amore, P. A. (1994) *Invest. Ophthalmol. Vis. Sci.* **35,** 3974–3979.
15. Wakasugi, K., Slike, B. M., Hood, J., Otani, A., Ewalt, K. L., Friedlander, M., Cheresh, D. & Schimmel, P. (2002) *Proc. Natl. Acad. Sci. USA* **99,** 173–177.
16. Rubin, B. Y., Anderson, S. L., Xing, L., Powell, R. J. & Tate, W. P. (1991) *J. Biol. Chem.* **266,** 24245–24248.
17. Fleckner, J., Rasmussen, H. H. & Justesen, J. (1991) *Proc. Natl. Acad. Sci. USA* **88,** 11520–11524.
18. Honore, B., Leffers, H., Madsen, P. & Celis, J. E. (1993) *Eur. J. Biochem.* **218,** 421–430.
19. Reano, A., Richard, M. H., Denoroy, L., Viac, J., Benedetto, J. P. & Schmitt, D. (1993) *J. Invest. Dermatol.* **100,** 775–779.
20. Fleckner, J., Martensen, P. M., Tolstrup, A. B., Kjeldgaard, N. O. & Justesen, J. (1995) *Cytokine* **7,** 70–77.
21. Tolstrup, A. B., Bejder, A., Fleckner, J. & Justesen, J. (1995) *J. Biol. Chem.* **270,** 397–403.
22. Turpaev, K. T., Zakhariev, V. M., Sokolova, I. V., Narovlyansky, A. N., Amchenkova, A. M., Justesen, J. & Frolova, L. Y. (1996) *Eur. J. Biochem.* **240,** 732–737.
23. Shaw, A. C., Rossel Larsen, M., Roepstorff, P., Justesen, J., Christiansen, G. & Birkelund, S. (1999) *Electrophoresis* **20,** 984–993.
24. Aboagye-Mathiesen, G., Ebbesen, P., von der Maase, H. & Celis, J. E. (1999) *Electrophoresis* **20,** 344–348.
25. Yuan, W., Collado-Hidalgo, A., Yufit, T., Taylor, M. & Varga, J. (1998) *J. Cell Physiol.* **177,** 174–186.
26. Brooks, P. C., Montgomery, A. M. & Cheresh, D. A. (1999) *Methods Mol. Biol.* **129,** 257–269.
27. Eliceiri, B. P., Paul, R., Schwartzberg, P. L., Hood, J. D., Leng, J. & Cheresh, D. A. (1999) *Mol. Cell* **4,** 915–924.
28. Bailey, A. J., Sloane, J. P., Trickey, B. S. & Ormerod, M. G. (1982) *J. Pathol.* **137,** 13–23.
29. Friedlander, M., Theesfeld, C. L., Sugita, M., Fruttiger, M., Thomas, M. A., Chang, S. & Cheresh, D. A. (1996) *Proc. Natl. Acad. Sci. USA* **93,** 9764–9769.
30. Ashton, N. (1970) *Br. Med. Bull.* **26,** 103–106.
31. Alon, T., Hemo, I., Itin, A., Pe'er, J., Stone, J. & Keshet, E. (1995) *Nat. Med.* **1,** 1024–1028.
32. Stone, J., Itin, A., Alon, T., Pe'er, J., Gnessin, H., Chan-Ling, T. & Keshet, E. (1995) *J. Neurosci.* **15,** 4738–4747.
33. Park, S. G., Jung, K. H., Lee, J. S., Jo, Y. J., Motegi, H., Kim, S. & Shiba, K. (1999) *J. Biol. Chem.* **274,** 16673–16676.
34. Norcum, M. T. & Warrington, J. A. (2000) *J. Biol. Chem.* **275,** 17921–17924.
35. Kao, J., Ryan, J., Brett, G., Chen, J., Shen, H., Fan, Y. G., Godman, G., Familletti, P. C., Wang, F., Pan, Y. C., *et al.* (1992) *J. Biol. Chem.* **267,** 20239–20247.

36. Kao, J., Houck, K., Fan, Y., Haehnel, I., Libutti, S. K., Kayton, M. L., Grikscheit, T., Chabot, J., Nowygrod, R., Greenberg, S., *et al.* (1994) *J. Biol. Chem.* **269,** 25106–25119.
37. Quevillon, S., Agou, F., Robinson, J. C. & Mirande, M. (1997) *J. Biol. Chem.* **272,** 32573–32579.
38. Tas, M. P., Houghton, J., Jakobsen, A. M., Tolmachova, T., Carmichael, J. & Murray, J. C. (1997) *Cytokine* **9,** 535–539.
39. Knies, U. E., Behrensdorf, H. A., Mitchell, C. A., Deutsch, U., Risau, W., Drexler, H. C. & Clauss, M. (1998) *Proc. Natl. Acad. Sci. USA* **95,** 12322–12327.
40. Schwarz, M. A., Kandel, J., Brett, J., Li, J., Hayward, J., Schwarz, R. E., Chappey, O., Wautier, J. L., Chabot, J., Lo Gerfo, P. & Stern, D. (1999) *J. Exp. Med.* **190,** 341–354.
41. Barnett, G., Jakobsen, A. M., Tas, M., Rice, K., Carmichael, J. & Murray, J. C. (2000) *Cancer Res.* **60,** 2850–2857.
42. Schwarz, M., Lee, M., Zhang, F., Zhao, J., Jin, Y., Smith, S., Bhuva, J., Stern, D., Warburton, D. & Starnes, V. (1999) *Am. J. Physiol.* **276,** L365–L375.
43. Folkman, J. (1995) *Nat. Med.* **1,** 27–31.
44. Aiello, L. P. (1997) *Ophthalmic Res.* **29,** 354–362.
45. Griffioen, A. W. & Molema, G. (2000) *Pharmacol. Rev.* **52,** 237–368.
46. Miller, J. W., Adamis, A. P., Shima, D. T., D'Amore, P. A., Moulton, R. S., O'Reilly, M. S., Folkman, J., Dvorak, H. F., Brown, L. F., Berse, B., *et al.* (1994) *Am. J. Pathol.* **145,** 574–584.
47. Hellstrom, A., Perruzzi, C., Ju, M., Engstrom, E., Hard, A. L., Liu, J. L., Albertsson-Wikland, K., Carlsson, B., Niklasson, A., Sjodell, L., *et al.* (2001) *Proc. Natl. Acad. Sci. USA* **98,** 5804–5808. (First Published May 1, 2001; 10.1073/pnas.101113998)
48. Ingber, D., Fujita, T., Kishimoto, S., Sudo, K., Kanamaru, T., Brem, H. & Folkman, J. (1990) *Nature (London)* **348,** 555–557.
49. Rastinejad, F., Polverini, P. J. & Bouck, N. P. (1989) *Cell* **56,** 345–355.
50. Brooks, P. C., Clark, R. A. & Cheresh, D. A. (1994) *Science* **264,** 569–571.
51. Bateman, A., Birney, E., Durbin, R., Eddy, S. R., Howe, K. L. & Sonnhammer, E. L. (2000) *Nucleic Acids Res*. **28,** 263–266.
52. Ge, Q., Trieu, E. P. & Targoff, I. N. (1994) *J. Biol. Chem.* **269,** 28790–28797.
53. Hirakata, M., Suwa, A., Takeda, Y., Matsuoka, Y., Irimajiri, S., Targoff, I. N., Hardin, J. A. & Craft, J. (1996) *Arthritis Rheum* **39,** 146–151.
54. Fett, R. & Knippers, R. (1991) *J. Biol. Chem.* **266,** 1448–1455.
55. Tsui, F. W. & Siminovitch, L. (1987) *Nucleic Acids Res.* **15,** 3349–3367.
56. Frolova, L. Y., Sudomoina, M. A., Grigorieva, A. Y., Zinovieva, O. L. & Kisselev, L. (1991) *Gene* **109,** 291–296.